VOL. 14, NO. 5, MARCH 2019 ISSN 1819-6608
ARPN Journal of Engineering and Applied Sciences

www.arpnjournals.com

KINEMATIC, DYNAMIC MODELING AND DESIGN OF A P-D CONTROLLER FOR A FOUR-DEGREE-OF-FREEDOM ROBOT

Juan Gabriel Jimenez Perdomo[1], Oscar Andres Otalora Castro[2], Jorge Luis Aroca Trujillo[3] and Ruthber Rodriguez Serrezuela[3]
[1]Faculty of Business Administration, Corporación Universitaria Minuto de Dios, Neiva, Colombia
[2]Electronic Engineering, Universidad Antonio Nariño-UAN
[3]Industrial Engineering, Corporación Universitaria del Huila, CORHUILA
E-Mail: ruthber.rodriguez@corhuila.edu.co

ABSTRACT

In this work the kinematic and dynamic modeling of an industrial robot with four degrees of freedom is obtained. The kinematic model is found and validated through the Matlab software. For the design of the controller, a proportional and derivative feedback (P-D) is selected to determine the control signal, generating a linear PD driver feedback linearization type using Matlab / Simulink. The main current bibliographical references for the kinematic and dynamic analysis of industrial robots are taken into account for this work.

Keywords: kinematics, dynamics, DH parameters, P-D control.

INTRODUCTION

Any process can be manipulated and at the same time its reaction can be calculated in a quantitative or qualitative way. This reaction can be named as a system or plant, and at the same time it is possible to use control tasks.

Control is applicable in some aspects of daily life. In fact, the human body is a system of instrumentation and control par excellence. For example, taking a glass with your hand involves control actions, which is an extremely complex mathematical illustration. The realization of this action begins with a mental photograph of the glass in the hand (known as the condition of stability), and thanks to the help of the eyes, a photograph of the spatial perspective of the glass is taken (that is, the reference) as well as that of the spatial position of the hand (current state of the system). The brain processes and sends these two images towards the bundled muscles in such arm movement. Electric excitations are necessary to take the glass, so everything is done almost involuntarily.

The control from the point of view of electronic or electrical circuits helps a lot to the stability of some variables that perform a job. For example: sources of direct current, inverters, or mechanical control systems such as the damping of a car or a motor.

In light of the above, two main ideas are concluded: 1) for a control to exist, there must be a plant where to apply it, and (2) the actions of such control seek the stability of the system in such a way that it is important to know the behaviour of the plant to develop a control plant, which is manifested in the transfer function (relationship between input and output) or in state space models (relationship of the variables that intervene in a system). The two models achieved by the application of physical laws will be the essence of study, along with the design of the control. [1]

A control system has as a basic scheme as shown in Figure-1.

Closed loop plant

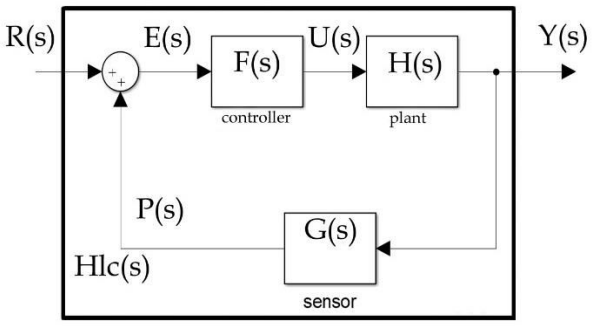

Figure-1. Basic outline of a control system.

In a feedback control loop, as shown in Figure-1, the control operations are executed with an instrument known as a controller. It has control modes or actions that are executed on the error signal e (t). The desired value of the controlled variable r (t) and its value y (t) is the difference of the error mentioned before. They are constantly expected specialties of the control system. Taken as a controlled variable, the controlled system has a new desired value in question that changes, or returns to its wanted value in the presence of a disturbance z (t), in the minimum possible time, with inappreciable oscillations and mistakes. The way the controller executes depends on the value of the parameters and their structure. [2]

In order to increase the stability of the system by improving the control, the P-D controller is used, which has the ability to predict the future error of the response of said system. If wanted to obviate the artifacts of unexpected change in the value of the error signal, the derivative is taken from the output response of the system variable instead of the error signal. Model D is set to be proportional to the exchange of the output variable, which prevents sudden changes in the control output as a result of unforeseen changes in the error signal. At the same

time, D directly increases the noise of the process, so the D-only control is not used. [3]

The derivative controller is opposed to deviations of the input signal, with a response that is proportional to the speed with which they occur.

Considering that:

y(t) = Differential output.

e(t) = Error (difference between measurement and set point [SP] The SP is nothing other than the desired level at which we want the system to return)

Td = Differential time, used to give more or less importance to the derivative action.

The output of this regulator is:

$$y(t) = t_d * \frac{de(t)}{dt}$$

In the Laplace domain, it will be:

$$Y(s) = T_d * s * E(s)$$

So its transfer function will be:

$$G(s) = \frac{Y(s)}{E(s)} = T_d * s$$

If the input variable is constant, it does not end the result of the differential regulator. When the alterations of the input are instantaneous, the speed of variation will be very high, and, consequently, the result will be abruptly from the differential regulator. Therefore, its use is not advisable.

The differential regulator does not proceed exclusively (this is why it has not been explained separately as we have done with the integral. Nevertheless, the pure integral does not exist either), which is continuously associated with the action of a proportional regulator (and that is why we talk about regulator PD). From the control block, its output expresses the following equation:

$$y(t) = K_p * t_d * \frac{de(t)}{dt} + k_p * e(t)$$

Kp and Td are applicable measures of the system.

Td is referred to derivative time, which is a measure of the speed of a PD controller that replaces a swap in the regulated variable, compared to a pure controller P.

In the Laplace domain, it will be:

$$Y(s) = K_p * T_d * s * E(s) + k_p * E(s)$$

Consequently, the transfer function of the PD control block will be:

$$G(s) = \frac{Y(s)}{E(s)} = K_p * (T_d * s + 1)$$

KYNETMATIC MODEL

As observed in Figure-2, a symbolic representation of the robotic arm, in this representation 5 precise reference frames emerge to form the arm. Notice that the arm has four freedom degrees, due to its four rotary joints and 5 links, counting the base. This is called an angular or articulated manipulator, which has a spherical working area.

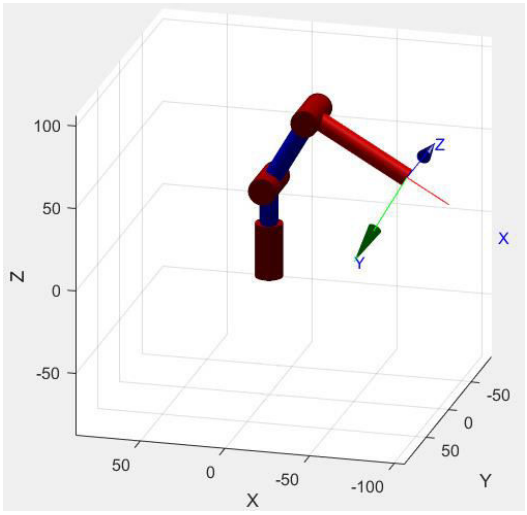

Figure-2. Symbolic representation of the robotic arm and reference frames assignment.

According to the DH agreement, reference frames are placed considering the following guidelines:

a) Joints are numbered from i = 1 to n, i being, the ith joint.

b) The zi axes are placed along the following joint i+ 1.

c) If $zi$and zi-1 are intercepted, the source of the frame xi yizi is placed into that point. This happens in x0 y0z0 y xi yizi frames as well as in frames x2 y2z2 y x3 y3z3.

d) Axis xi is taken along the common normal among the zi and zi-1 with direction from the joint i towards i +1.

e) Axis yi is taken in a way that the frame is completed.

f) For the base (frame x0 y0z0) only the direction of the z0 axis is specified and x0 y0z0 are chosen conveniently.

g) For the last link, there is no $i + 1$ frame. In general, joint n is rotatory and axis zn. is selected aligned with zn-1.

Four standards of the manipulator are obtained parting from these reference frames:

- ai Link length: Distance between axes zi-1 and zi along axisxi .
- Joint Distance di: It is the distance between axes xi-1 and xi along the zi-1 axis.
- Joint angle θi: The torque required of the axis xi-1 on zi-1 to be parallel to xi. Right-hand rule is used to know the direction.
- Torsion angle αi: torque required of the zi-1 on xi to be parallel to zi.

In Table-1 specific data of the robotic arm are shown, which represent link dimensions and torsion angles in joints 1 and 2, and joints 3 and 4 respectively. Let it be noted that in each row of the table there is only one variable, in this case, it is the angle of rotation of each joint θi.

Table-1. DH parameters for a robotic arm.

Link(i)	ai (cm)	αi	di (cm)	θi
1	a1 =0	α1 =π/2	d1 =0	θ1
2	a2 =13	α2 =0	d2 =0	θ2
3	a3 =0	α3 =π/2	d3 =0	θ3
4	a4 =0	α4 =0	d4 =17	θ4

A. Direct position kinematic model

The position of the PT can be known by simplifying the design shown in Figure-2; as it is observed joint 4 is not fundamental and does not affect the final position of the manipulator.

Next, in Figure-3, Table-2 is observed with the related parameters and the new representation.

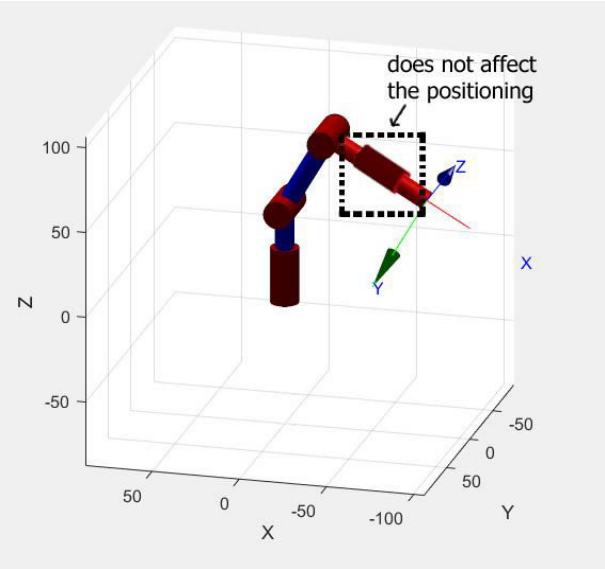

Figure-3. Symbolic representation of the robotic arm.

What is observed in Table-2 is reduced in a row which is related to Table-1, which will reflect the number of instructions to execute in order to calculate the direct kinematics of the manipulator.

If joint 4 is removed there will not be a torsion angle between 2 and 3 and its articulation distance d4 is transformed along the link α3.

Table-2. Simplified DH parameters.

Link(i)	ai (cm)	αi	di (cm)	θi
1	a1 =0	α1 =π/2	d1 =0	θ1
2	a2 =13	α2 =0	d2 =0	θ2
3	a3 =20	α3 =0	d3 =0	θ3

The DH convention indicates that each row in Table-2 must be transformed into a homogeneous matrix A_i^(i-1) where the composition of 4 homogeneous basic matrices is acquired according to the following equation:

$$A_i^{i-1} = R_{z,\theta_i} T_{z,d_i} T_{x,a_i} R_{x,a_i} \quad (1)$$

Where:

$$R_{z,\theta_i} = \begin{bmatrix} cos\theta_i & -sin\theta_i & 0 & 0 \\ sin\theta_i & cos\theta_i & 0 & 0 \\ 0 & 0 & 1 & 0 \\ 0 & 0 & 0 & 1 \end{bmatrix}$$

$$T_{z,d_i} = \begin{bmatrix} 1 & 0 & 0 & 0 \\ 0 & 1 & 0 & 0 \\ 0 & 0 & 1 & d_i \\ 0 & 0 & 0 & 1 \end{bmatrix}$$

$$T_{x,a_i} = \begin{bmatrix} 1 & 0 & 0 & a_i \\ 0 & 1 & 0 & 0 \\ 0 & 0 & 1 & 0 \\ 0 & 0 & 0 & 1 \end{bmatrix}$$

$$R_{x,\alpha_i} = \begin{bmatrix} 1 & 0 & 00 \\ cos\alpha_i & -sin\alpha_i & 00 \\ sin\alpha_i & cos\alpha_i & 10 \\ 0 & 0 & 01 \end{bmatrix}$$

Matrix R_{z,θ_i} indicates rotation in the z axis with angle θ_i, the T_{z,d_i} matrix shows movement on the z axis with a d_i distance, the matrix R_{x,α_i} shows rotation in axis x with an α_i angle, whereas matrix T_{x,a_i} shows movement on the x axis with a a_i distance. The homogeneous matrix (equation 3) is obtained by performing matrix operations, where θ_i is the joint variable and the other parameters are constant.

$$A_i^{i-1} = \begin{bmatrix} cos\theta_i & -sin\theta_i cos\alpha_i & sin\theta_i sin\alpha_i & \alpha_i cos\theta_i \\ sin\theta_i & cos\theta_i cos\alpha_i & -cos\theta_i sin\alpha_i \alpha_i sin\theta_i \\ 0 & 0 & 1 & d_i \\ 0 & 0 & 0 & 1 \end{bmatrix} \quad (2)$$

Matrices associated with each link are obtained from the previous equation.

$$A_1^0 = \begin{bmatrix} cos\theta_1 & 0 & sin\theta_1 & 0 \\ sin\theta_1 & 0 & -cos\theta_1 & 0 \\ 0 & 0 & 1 & 0 \\ 0 & 0 & 0 & 1 \end{bmatrix}$$

$$A_2^1 = \begin{bmatrix} cos\theta_2 & -sin\theta_2 & 0a_2 cos\theta_2 \\ sin\theta_2 & cos\theta_2 & 0a_2 sin\theta_2 \\ 0 & 0 & 1 & 0 \\ 0 & 0 & 0 & 1 \end{bmatrix}$$

$$A_3^2 = \begin{bmatrix} cos\theta_3 & -sin\theta_3 & 0a_3 cos\theta_3 \\ sin\theta_3 & cos\theta_3 & 0a_3 sin\theta_3 \\ 0 & 0 & 1 & 0 \\ 0 & 0 & 0 & 1 \end{bmatrix}$$

The first result A_1^0 0 manifests information about the location of frames x1 y1z1. Regarding the base frame. Both frames are incorporated one on top of the other, but with an uneven alignment. The second frame is exported with a distance of $[a_2 cos\theta_2 a_2 sin\theta_2\ 0]^T$ regarding the first frame and so on, with a different distribution of this one.

Finally, the frame x3 y3z3 is exported to $[a_3 cos\theta_3 a_3 sin\theta_3\ 0]$T. with respect to the second frame, and with a different alignment.

The composition of these homogeneous matrices according to the equation (4) allows finding coordinates of the PT manipulator on the basis of the reference frame and therefore the position of this point with respect to the base.

$$T_3^0(q) = A_1^0 A_2^1 A_3^2 \quad (3)$$

Vector q = $[\theta_1\theta_2\theta_3]$ T is called a generalized coordinate vector. The result of this operation is: Vector q =

$$T_3^0(q) = \begin{bmatrix} c_1c_2c_3 - c_1s_2s_3 & -c_1c_2s_3 - c_1c_3s_2 & s_1\ a_2c_1c_2 - a_3c_1s_2s_3 + a_3c_1c_2c_3 \\ c_2c_3s_1 - s_1s_2s_3 & -c_2s_1s_3 - c_3s_1s_3 & -c_1a_2c_2s_1 - a_3s_1s_2s_3 + a_3c_2c_3s_1 \\ c_2s_3 + c_3s_2 & c_2c_3 - s_2s_3 & 1\quad a_2s_2 - a_3c_2s_3 + a_3c_3s_2 \\ 0 & 0 & 0\quad 1 \end{bmatrix} \quad (4)$$

The direct kinematic model is obtained Where $cos\theta_i = c_i$ and $sin\theta_i = s_i$ of matrix (5). PT position is:

$$O_3^0 = \begin{bmatrix} p_x \\ p_y \\ Pz \end{bmatrix} = \begin{bmatrix} a_2c_1c_2 - a_3c_1s_2s_3 + a_3c_1c_2c_3 \\ a_2c_2s_1 - a_3s_1s_2s_3 + a_3c_2c_3s_1 \\ a_2s_2 - a_3c_2s_3 + a_3c_3s_2 \\ 1 \end{bmatrix} \quad (5)$$

Whereas the final direction with respect to the base is given by the rotation matrix:

$$R_3^0 = \begin{bmatrix} p_x \\ p_y \\ Pz \end{bmatrix} = \begin{bmatrix} c_1c_2c_3 - c_1s_2s_3 & -c_1c_2s_3 - c_1c_3s_2 & s_1 \\ c_2c_3s_1 - s_1s_2s_3 & -c_2s_1s_3 - c_3s_1s_3 & -c_1 \\ c_2s_3 + c_3s_2 & c_2c_3 - s_2s_3 & 1 \\ 0 & 0 & 0 \end{bmatrix} \quad (6)$$

B. Inverse kinematic model of position

Dispelling the inverse kinematic model, i.e., obtaining the values of qO_3^0 0, implies solving the system of three equations and three unknowns shown in (6). However, these trigonometric equations are not easyto resolve since most of the times there is more than one possible solution, and even infinite solutions. The geometrical method described below applies to the robotic arm.

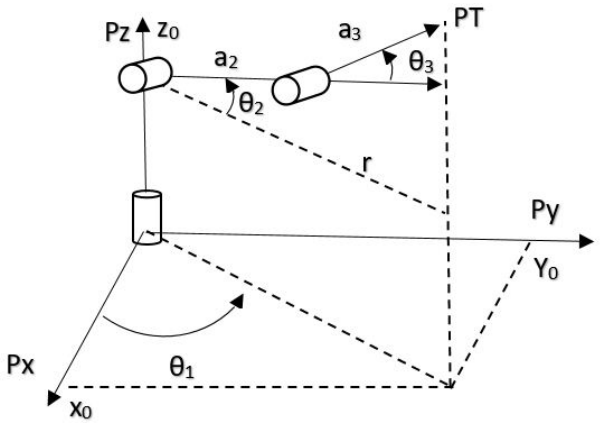

Figure-4. Geometric representation of the robotic arm.

From Figure-4 it is observed that the angle $\theta_i$is obtained from the trigonometric equation:

$$\theta_i = tan^{-1}\left(\frac{Py}{Px}\right), \forall\, Py \neq 0, Px \neq 0 \quad (7)$$

If px and py are null, you get infinite solutions forθ_1. This indicates that the PT is located along the z-axis of the base. In this case you can choose an arbitrary value or just hold the previous value.

To calculate any angle θ, instead of using the equation$\theta = tan^{-1}\left(\frac{y}{Px}\right)$, it is more practical to use the function:

$$\theta = atan2(y, x) \quad (8)$$

This feature is called arc-tangent of two arguments and uses the signs of x and y to automatically select the quadrant of the angleθ, for example, $a$tan2(1, −1) =-π/4, while $a$tan2(−1,1) = + 3π/4. Most of the mathematical aids and libraries of modern programming languages have it. Then:

$$\theta = atan2(Py, Px) \quad (9)$$

From Figure-4 and the Pythagorean Theorem the following equation arises:

$$r^2 = p_x^2 + p_y^2 \quad (10)$$

To obtain the values of θ2 and θ3, the geometric construction, which is shown in Figure-5, is used. The same shows two possible positions of the robotic arm to reach the same final position.

Para obtener los valores deθ2 y θ3 se utiliza la construcción geométrica que se muestra en la Figure-5. La misma muestra dos posibles posturas del brazo robótico para alcanzar la misma posición final.

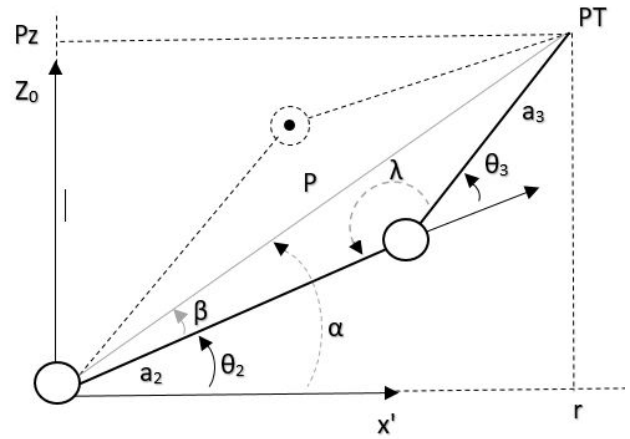

Figure-5. Positions of the robotic arm with the same PT.

A geometric analysis results in the following relationships:

$$\lambda = \pi - \theta_3 \quad (11)$$

According to the Pythagorean Theorem:

$$p^2 = r^2 + p_z^2 = p_x^2 + p_y^2 + p_z^2 \quad (12)$$

Applying the law of cosines and (11) is

$$p^2 = a_2^2 + a_3^2 - 2a_2a_3cos\lambda = a_2^2 + a_3^2 + 2a_2a_3cos\theta_3 \quad (13)$$

$$a_3^2 = p^2 + a_2^2 - 2Pa_2cos\beta \quad (14)$$

Clearing cosθ_3 in (13) and combining with (12) it is obtained:

$$cos\theta_3 = \frac{p_x^2 + p_y^2 + p_z^2 - (a_2^2 + a_3^2)}{2a_2a_3} \equiv C \quad (15)$$

$$sin\theta_3 = \pm\sqrt{(1-c)^2} \quad (16)$$

Combining (15) and (16) in (8) it is obtained:

$$\theta_3 = atan2(\pm\sqrt{(1-c)^2}, C) \quad (17)$$

If the positive value of$\theta_3$is taken the position below shown in Figure-5 is selected. On the other hand, if the value of$\theta_3$is taken with negative sign the top position is selected.

The value ofθ_2 is obtained:

$$\theta_2 = \begin{cases} \alpha - \beta & si\theta_3 > 0 \\ \alpha + \beta & si\theta_3 < 0 \\ \alpha & si\theta_3 = 0 \end{cases} \quad (18)$$

Where$\beta$is calculatedfrom (12) and (14)?

$$\beta = cos^{-1}\left(\frac{p_x^2 + p_y^2 + p_z^2 + a_2^2 - a_3^2)}{2a_2\sqrt{p_x^2 + p_y^2 + p_z^2}}\right) \quad (19)$$

And$\alpha$is calculated using (8) and (10):

$$\alpha = atan2(p_z, r) = atan2\left(p_z, \sqrt{p_y^2 + p_x^2}\right) \quad (20)$$

Equations (9), (17) and (18) make up the kinematic model reverse position for the robotic arm. These equations are based on the constant parameters of the manipulatora_2,a_3 and the PT given by the coordenates (p_x, p_y, p_z).

DYNAMIC MODEL

The method used to obtain the dynamic model of the robotic manipulator is based on the so-called equations of Euler-Lagrange, which are presented below:

$$\frac{d}{dt}\frac{\partial L}{\partial \dot{q}_i} - \frac{\partial L}{\partial q_i} = \tau \quad (21)$$

$$L = K - P \quad (22)$$

Where,$q_i$are the generalized coordinates, τ vector of forces or pairs applied to links, while K and P are the kinetic energy and the potential energy of the manipulator, respectively.

The equation (23) shows that the kinetic energy has a component of linear translation Kl plusanother rotational component$K$r.

$$K=Kl+ Kr \quad (23)$$

From the point of view Kl vector it is obtained as:

$$k_l = \frac{1}{2}m\begin{bmatrix}v_x v_y v_z\end{bmatrix}\begin{bmatrix}v_x\\v_y\\v_z\end{bmatrix} = \frac{1}{2}mv^T v \quad (24)$$

While Kris obtained as:

$$k_l = \frac{1}{2}m\begin{bmatrix}v_x v_y v_z\end{bmatrix}\begin{bmatrix}v_x\\v_y\\v_z\end{bmatrix} = \frac{1}{2}mv^T v \quad (25)$$

Being $m$the mass of the body and$I$the matrix (3×3) called the tensor dof inertia.

Each element of the kynematic chain of the robotic arm provides translational and rotational energy to the manipulator. For the analysisthe mass of links concentrated in its center of gravity is considered as shown in Figure 6. The tensor of inertia I is referred to this point, too.

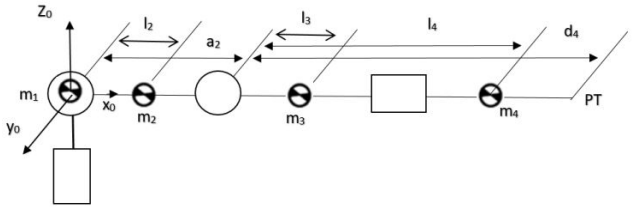

Figure-6. Symbolic representation of the robotic arm with their centers of mass.

Then the energy of the third link is analyzed and it can be generalized the result for the rest of the links from it. The equation (26) obtains the linear and angular speed of the center of mass of the third link in vector form. Note that the fourth link does not provide energy of translation or rotation to the third, while the first two do. Therefore, the Jacobian matrix only considers non-zero terms until the third link.

$$\begin{bmatrix}\frac{V_3}{W_3}\end{bmatrix} = \begin{bmatrix}J_{v1} & J_{v2} & J_{v3}\,0\\ J_{w1} & J_{w2} & J_{w3}\,0\end{bmatrix}\begin{bmatrix}w_1^0\\w_2^1\\w_3^2\\w_4^3\end{bmatrix} = \begin{bmatrix}J_{v13}\\J_{w13}\end{bmatrix}\dot{q} \quad (26)$$

Equation (27) allows calculating the total power of the link.

$$k_3 = \frac{1}{2}m_3 v_3^T v_3 + \frac{1}{2}w_3^T R_3^0 I_3 (R_3^0)^T w_3 \quad (27)$$

Product$R_3^0 I_3 (R_3^0)^T$allows expressing the tensor of inertia with respect to the reference frame at the base. When substituting in (27) variables$v_3$and$w_3$in terms of the generalized coordinates is:

$$\mathrm{k_3} = \frac{1}{2}\mathrm{m_3(J_{v13}\dot{q})^T(J_{v13}\dot{q})} + \frac{1}{2}\mathrm{(J_{w13}\dot{q})^T R_3^0 I_3 (R_3^0)^T (J_{w13}\dot{q})} \quad (28)$$

The potential energy of the third link in vector form is expressed:

$$P_3 = -m_3\begin{bmatrix}0 & 0 & -g\end{bmatrix}\begin{bmatrix}P_{c3x}\\P_{c3y}\\P_{c3z}\end{bmatrix} = -m_3 g^T P_{c3} \quad (29)$$

Where $g$is the acceleration of gravity and the pointP_{c3} refers to the position in space of the center of gravity of the third link with respect to the base.Gravity always acts referred to the axis z of the base frame.

In the same way we get kinetic energy and potential for every link, resulting in expressions:

$$K = \frac{1}{2}\sum_{i=1}^{4} m_i (J_{v1}\dot{q})^T (J_{v1i}\dot{q}) + (J_{w1i}\dot{q})^T R_i^0 I_i (R_i^0)^T (J_{w1}\dot{q}) \quad (30)$$

$$P = \sum_{i=1}^{4} -m_i\, g^T P_{ci} \quad (31)$$

Equation (54) can be written in a compact form:

$$K = \frac{1}{2}\dot{q}^T[\sum_{i=1}^{4} m_i J_{v1i}^T J_{v1i} + J_{w1i}^T R_i^0 I_i (R_i^0)^T J_{w1i}]\dot{q} = \dot{q}^T D(q)\dot{q} \quad (32)$$

Where is D a symmetric matrix of 4×4 which is known as inertia matrix. Substituting (31) and (32) in (22) and then (21) it is possible to get the dynamic model of the robotic arm. The general solution of the equation (21) for robotic manipulators is expressed as a function of three terms:

$$D(q)q + C(q,\dot{q})\ddot{q} + G(q) = \tau \quad (33)$$

Where:

D: matrix of inertia formed by elements $\mathrm{d_{ij}}$, $1 \leqslant i \leqslant 4$; $1 \leqslant j \leqslant 4$

C: matrix of terms of Coriolis and centrifugal forces (4 × 4). Related to the physical interaction of the links.

Its elements $\mathrm{c_{kj}}$, $1 \leqslant k \leqslant 4$; $1 \leqslant j \leqslant 4$ are calculated as follows:

$$\mathrm{c_{kj}} = \sum_{i=1}^{4} \mathrm{c_{ijk}}(q)\dot{q} \quad (34)$$

The terms c_{ijk} are called Christoffel symbols and the way to obtain them is:

$$c_{ijk} = \frac{1}{2}\left\{\frac{\partial d_{kj}}{\partial q_i} + \frac{\partial d_{ki}}{\partial q_j} - \frac{\partial d_{ij}}{\partial q_k}\right\} \quad (35)$$

G: gravity vector (4 × 1). Its elements g_i; $1 \leqslant i \leqslant 4$, are obtained:

$$g_i = \frac{\partial P}{\partial q_i} \quad (36)$$

The dynamic model of the robotic arm was obtained with the help of software Matlab. $D(q)$ is for the inertia matrix:

$$\begin{aligned}
d_{11} &= I_{1y} + I_{2x} + I_{3z} + I_{4z} + \left(I_{2y} - I_{2x} + l_2^2 m_2\right)c_2^2 \\
&\quad + \left(I_{3x}c_3^2 + I_{3y}s_3^2 + I_{4x}c_4^2 + I_{4x}c_4^2 + I_{3z}\right. \\
&\quad \left. - I_{4z}\right)s_{23}^2 + m_3(I_3 s_{23} + a_2 c_2)^2 \\
&\quad + m_4(I_4 s_{23} + a_2 c_2)^2 \\
d_{12} &= d_{21} = \left(I_{3x} - I_{3y}\right)c_3 s_3 s_{23} + (I_{4x} - I_{4y})c_4 s_4 s_{23} \\
d_{13} &= d_{31} = \left(I_{3x} - I_{3y}\right)c_3 s_3 s_{23} + (I_{4x} - I_{4y})c_4 s_4 s_{23} \\
d_{14} &= d_{41} = -I_{4z}c_{23} \\
d_{22} &= I_{2z} + I_{3x}s_3^2 + I_{4x}s_4^2 + I_{3y}c_3^2 + I_{4y}c_4^2 + m_2 l_2^2 + c_2^2 \\
&\quad + m_3(l_3^2 + 2a_2 l_3 s_3 + a_2^2) \\
&\quad + m_3(a_2^2 + 2a_2 l_4 s_3 + d_4^2) \\
d_{23} &= I_{3y} + I_{4y}c_4^2 + I_{3x}s_3^2 + I_{4x}s_4^2 + m_4 l_4^2 + m_3 l_3^2 \\
&\quad + a_2 s_3(l_4 m_4 + l_3 m_3) \\
d_{24} &= d_{42} = 0 \\
d_{33} &= I_{3y}c_3^2 + I_{4y}c_4^2 + I_{3x}s_3^2 + I_{4x}s_4^2 + m_4 l_4^2 + m_3 l_3^2 \\
d_{34} &= d_{43} = 0 \\
d_{44} &= I_{4z} = 0
\end{aligned}$$

The Christoffel symbols are:

$$\begin{aligned}
c_{114} &= (I_{4y} - I_{4x})s_{23}^2 c_4 s_4 \\
c_{121} &= c_{112} \\
c_{122} &= ((I_{3x} - I_{3y})c_3 s_3 + (I_{4x} - I_{4y})c_4 s_4)c_{23} \\
c_{123} &= (I_{3y} - I_{3x})\left(\frac{1}{2}s_{23} + c_3 s_2 + 2c_3^2 s_{23}\right) + +(I_{4x} \\
&\quad - I_{4y})c_4 s_4 c_{23} \\
c_{124} &= \frac{1}{2}(I_{4y} - I_{4x} + I_{4z} + (I_{4y} - I_{4x})c_4^2)s_{23} \\
c_{131} &= c_{113} \\
c_{132} &= c_{123} \\
c_{133} &= (I_{3y} - I_{3x})(s_{23} + c_3 s_2 + 3c_3^2 s_{23}) + (I_{4x} \\
&\quad - I_{4y})c_4^2 c_4 s_4 c_{23} \\
c_{134} &= c_{124} \\
c_{141} &= c_{114} \\
c_{142} &= c_{124} \\
c_{143} &= c_{134} \\
c_{211} &= -c_{112} \\
c_{213} &= \frac{1}{2}(I_{3y} - I_{3x})s_{23}^2 s_{23} \\
c_{214} &= \frac{1}{2}(I_{4y} - I_{4x} - I_{4z} + 2(I_{4x} - I_{4y})c_2^2)s_{23} \\
c_{223} &= (I_{3x} - I_{3y})c_3 s_3 + a_2 c_3(I_4 m_4 + I_3 m_3) \\
c_{224} &= 2(I_{4x} - I_{4y})c_4 s_4 \\
c_{231} &= c_{213} \\
c_{232} &= c_{223} \\
c_{233} &= 2(I_{3x} - I_{3y})c_3 s_3 + a_2 c_3(I_4 m_4 + I_3 m_3) \\
c_{234} &= c_{224} \\
c_{241} &= c_{214} \\
c_{242} &= c_{224} \\
c_{243} &= c_{234} \\
c_{311} &= -c_{133} \\
c_{312} &= -c_{213} \\
c_{314} &= c_{214} \\
c_{321} &= c_{312} \\
c_{322} &= -c_{223} \\
c_{324} &= -c_{234} \\
c_{333} &= (I_{3x} - I_{3y})c_3 s_3 \\
c_{334} &= c_{234} \\
c_{341} &= c_{314} \\
c_{342} &= c_{324} \\
c_{343} &= c_{334} \\
c_{411} &= -c_{114} \\
c_{412} &= -c_{214} \\
c_{413} &= -c_{214} \\
c_{421} &= c_{412} \\
c_{422} &= -c_{224} \\
c_{423} &= -c_{234} \\
c_{431} &= c_{413} \\
c_{432} &= c_{423} \\
c_{433} &= -c_{334}
\end{aligned}$$

While the terms associated with the vector of gravity:

$$\begin{aligned}
g_1 &= 0 \\
g_2 &= gm_4(l_4 s_{23} + a_2 c_2) + gm_3(l_3 s_{23} + a_2 c_2) \\
&\quad + gl_2 m_2 c_2 \\
g_3 &= gs_{23}(l_4 m_4 + l_3 m_3) \\
g_1 &= 0
\end{aligned}$$

The variables l_i are the distance from the joint i to the centre of gravity of the i-th link. $s_{23} = \sin(\theta_2 + \theta_2)$, $c_{23} = \cos(\theta_2 + \theta_2)$. In addition, it has been considered that I_i inertia tensors associated with the center of mass of each link i have the general form:

$$I_i = \begin{bmatrix} I_{ix} & 0 & 0 \\ 0 & I_{iy} & 0 \\ 0 & 0 & I_{iz} \end{bmatrix} \quad (37)$$

Torque PD controller computed

Selecting a proportional and derivative feedback (PD) to determine $u_{(t)}$, the control signal, we generate the work of a PD computed torque controller:

$$\begin{aligned}
\tau &= M\left(\ddot{q} + K_v \dot{e} + K_p e\right) + N \\
\ddot{e} &= -k_v \dot{e} - k_p e
\end{aligned}$$

In the last expression, a follow-up dynamic error occurs, which is stable if the matrix k_v has large values and the matrix k_p is mathematically positively defined. The common is to select diagonal matrices in such a way that the stability of the system is assured for all the positive gains,

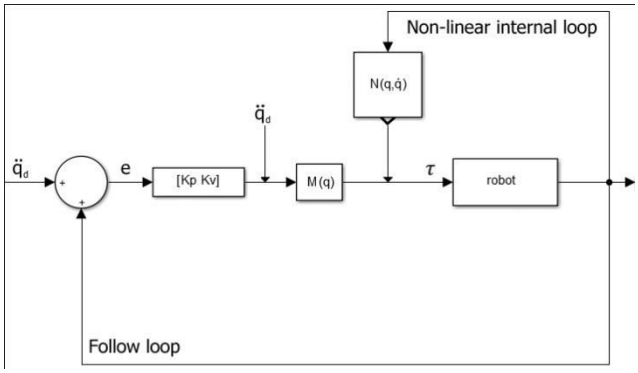

Figure-7. PD control diagram of computed torque.

$$q \equiv \begin{bmatrix} q \\ \dot{q} \end{bmatrix}, \quad e \equiv \begin{bmatrix} e \\ \dot{e} \end{bmatrix}, \quad y \quad q_d \equiv \begin{bmatrix} q_d \\ \dot{q_d} \end{bmatrix}$$

The computed torque PD controller has a multilayered structure, as shown in the figure. That is, a non-linear internal loop for linearization feedback and an external one for unit gain for tracking. Note that there are n outer loops, one for each articulation.

RESULTS

In Figure-8, it is seen that the angular errors in relation to the references practically disappear in a time less than 1 second, which shows that the model and the controller have been calculated appropriately.

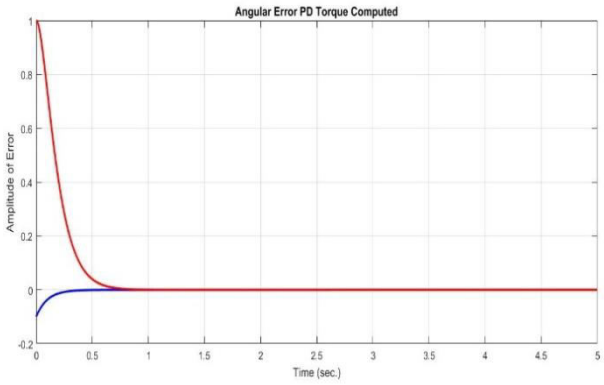

Figure-8. Angular PD error of computed torque.

In Figure-9, the same information is plotted, but on the real trajectories, and it can be seen that the desired ones (dotted lines) are reached by the real ones (continuous lines).

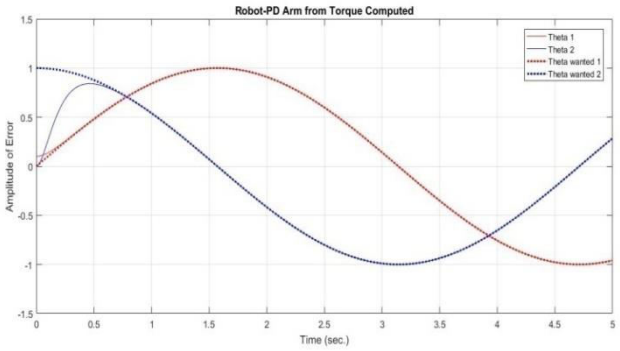

Figure-9. Real and desired trajectories.

In this case, Figure-10 presents the three-dimensional path of the desired trajectory (green in the simulation) and of the real one (red in the simulation). It is easy to appreciate that the actual trajectory covers almost the entire desired one, despite the non-linear characteristics of it.

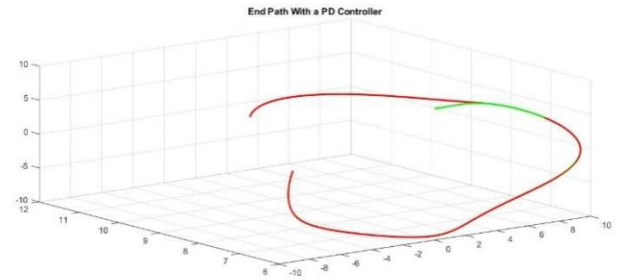

Figure-10. End trajectory with a PD controller.

In Figure-11, the real and desired trajectories on each of the Cartesian axes are presented.

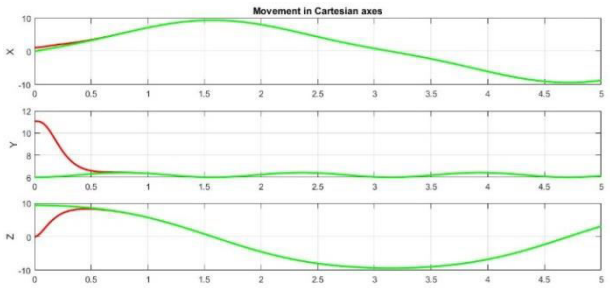

Figure-11. Movement in Cartesian axes.

CONCLUSIONS

The models found in this work can be implemented in the design of certain mechanisms and controllers of robots of similar morphology or equal degrees of freedom.

In Figure-8, you can see the response of the derivative controller, which anticipates the error signal itself. This type of controller is widely used in certain systems that must act with great speed, offering a response that causes the output to continuously vary in value.

The derivative regulator isn't usually implemented in isolation, since, for slow signals, the constant error produced in the output would be very large and if the control signal stopped acting for a long time the output would be seriously affected and would tend toward zero, which no control action would be taken.

The main advantage of this type of controller is that the speed of response of the control system increases.

REFERENCES

[1] Serrezuela R. R., Chavarro A. F. C., Cardozo M. A. T., Toquica A. L. & Martinez L. F. O. 2017. Kinematic modelling of a robotic arm manipulator using Matlab. ARPN Journal of Engineering and Applied Sciences. 12(7): 2037-2045.

[2] Rojas J. H. C., Serrezuela R. R., López J. A. Q. & Perdomo K. L. R. 2016. LQR hybrid approach control of a robotic arm two degrees of freedom. International Journal of Applied Engineering Research. 11(17): 9221-9228.

[3] Serrezuela R. R., Cardozo M. Á. T., Ardila D. L. & Perdomo C. A. C. 2018. A consistent methodology for the development of inverse and direct kinematics of robust industrial robots. ARPN Journal of Engineering and Applied Sciences. 13(01): 293-301.

[4] Aroca Trujillo J. L., Pérez-Ruiz A. & Rodriguez Serrezuela R. 2017. Generation and Control of Basic Geometric Trajectories for a Robot Manipulator Using CompactRIO®. Journal of Robotics.

[5] Trujillo J. L. A., Serrezuela R. R., Zarta J. R. & Ramos A. M. N. 2018. Direct and Inverse Kinematics of a Manipulator Robot of Five Degrees of Freedom Implemented in Embedded System-Compact RIO. Advanced Engineering Research and Applications, B. S. Ajaykumar and D. Sarkar Eds., Nueva Deli, India, Research India Publication. 405-419.

[6] Trujillo J. L. A., Serrezuela R. R., Azhmyakov V. & Zamora R. S. 2018. Kinematic Model of the Scorbot 4PC Manipulator Implemented in Matlab's Guide, Contemporary Engineering Sciences. 11(4): 183-199.

[7] Trujillo J. L. A., Zarta J. B. R. & Serrezuela R. R. 2018. Embedded system generating trajectories of a robot manipulator of five degrees of freedom (DOF), KnE Engineering. 3(1): 512-522.

[8] Azhmyakov V., Martinez J. C., Poznyak A. & Serrezuela R. R. 2015, July. Optimization of a class of nonlinear switched systems with fixed-levels control inputs. In American Control Conference (ACC), 2015 (pp. 1770-1775). IEEE.

[9] Azhmyakov V., Serrezuela R. R. & Trujillo L. G. 2014, October. Approximations based optimal control design for a class of switched dynamic systems. In Industrial Electronics Society, IECON 2014-40th Annual Conference of the IEEE (pp. 90-95). IEEE.

[10] Serrezuela R. R. & Chavarro A. F. C. 2016. Multivariable control alternatives for the prototype tower distillation and evaporation plant. International Journal of Applied Engineering Research. 11(8): 6039-6043.

[11] Azhmyakov V., Rodriguez Serrezuela R., Rios Gallardo A. M. & Gerardo Vargas W. 2014. An approximations based approach to optimal control of switched dynamic systems. Mathematical Problems in Engineering.

[12] Serrezuela R. R., Villar O. F., Zarta J. R. & Cuenca Y. H. 2016. The K-Exponential Matrix to solve systems of differential equations deformed. Global Journal of Pure and Applied Mathematics. 12(3): 1921-1945.

[13] Serrezuela R. R., Chavarro A. F. C., Cardozo M. A. T. & Zarta J. B. R. 2016. An Optimal Control Based Approach to Dynamics Autonomous Vehicle. International Journal of Applied Engineering Research. 11(16): 8841-8847.

[14] Montiel J. J. G., Serrezuela R. R. & Aranda E. A. 2017. Applied mathematics and demonstrations to the theory of optimal filters. Global Journal of Pure and Applied Mathematics. 13(2): 475-492.

[15] Serrezuela R. R., Chavarro A. F., Cardozo M. A., Caicedo A. G. R. & Cabrera C. A. 2017. Audio signals processing with digital filters implementation using MyDSP. Journal of engineering and applied sciences. 12(1).

[16] Benavides L. C. L., Pinilla L. A. C., López J. S. G. & Serrezuela R. R. 2018. Electrogenic Biodegradation Study of the Carbofuran Insecticide in Soil. International Journal of Applied Engineering Research. 13(3): 1776-1783.

[17] Serrezuela R. R., Cardozo M. Á. T., Ardila D. L. & Perdomo C. A. C. 2017. Design of a gas sensor based on the concept of digital interconnection IoT for the emergency broadcast system. Journal of Engineering and Applied Sciences. 12(22): 6352-6356.

[18] Serrezuela R. R., Trujillo J. A., Ramos A. N. & Zarta J. R. 2018. Applications Alternatives of Multivariable Control in the Tower Distillation and Evaporation Plant. Advanced Engineering Research and Applications, BS Ajaykumar and D. Sarkar Eds., Nueva Deli, India, Research India Publication. 452-465.

[19] Zarta J. R. & Serrezuela R. R. 2017. Solution of systems of differential equations deformed with K-Exponential Matrix. Taekyun Kim, Advanced Mathematics: Theory and applications. 189-204.

[20] Zarta J. B. R., Villar F. O., Serrezuela R. R. & Trujillo J. L. A. 2018. R-Deformed Mathematics. International Journal of Mathematical Analysis. 12(3): 121-135.

[21] Serrezuela R. R., Cardozo M. A. T. & Chavarro A. F. C. 2017. Design and Implementation of a PID Fuzzy Control for the Speed of a DC Motor. ARPN Journal of Engineering and Applied Sciences. 12(8): 2655-2660.

[22] Perdomo E. G., Cardozo M. Á. T., Fernández M. N. & Serrezuela R. R. 2018. Application and Automation of a Sequential Biological Reactor by Means of Programmable Logic Controller Using Petri Networks. Contemporary Engineering Sciences. 11(46): 2283-2295. https://doi.org/10.12988/ces.2018.84195

[23] Losada V. A. R., Bonilla E. P., Pinilla L. A. C. & Serrezuela R. R. 2018. Removal of Chromium in Wastewater from Tanneries Applying Bioremediation with Algae, Orange Peels and Citrus Pectin, Contemporary Engineering Sciences. 11(9): 433-449.

[24] Serrezuela R. R., Trujillo J. L. A., Delgado D. R., Benavides V. K. O., Zamora R. S. & Reyes E. M. 2018, September. Diseño e implementación de una prótesis de mano robótica antropomórfica subactuada. In Memorias de Congresos UTP. 1(1): 165-172.

[25] Ramos A. M. N., Trujillo J. L. A., Serrezuela R. R., & Zarta J. B. R. 2018. A Review of the Hotel Sector in the City of Neiva and the Improvement of its Competitiveness through Quality Management Systems. Chapter in Advanced Engineering Research and Applications, Nueva Deli, India, Research India Publication. 439-452.

[26] Serrezuel R. R., Cardozo M. Á. T., Benavides V. K. O. & Navarrete A. M. 2018, September. Control Híbrido Óptimo en una Modulación de Vector Espacial (SVM) para un Inversor de Potencia Electrica. In Memorias de Congresos UTP. 1(1): 137-143.

[27] Cardozo F. R. C., Pedraza N. A. P., Salazar A. L. P. & Serrezuela R. R. 2018. The Interaction Man-Computer and its Involvement in the Change of Paradigms of Education. Contemporary Engineering Sciences. 11(50): 2489-2501.

[28] Chávarro Cardozo F. R., Paque Salazar A. L. and Rodríguez Serrezuela R. 2018. Impact of Social Networks of Knowledge in Globalization. Contemporary Engineering Sciences. 11(50): 2475-2488.